Ab Initio Molecular Dynamics Simulations of Ionic Liquids

M. Thomas, I. Sancho Sanz, O. Hollóczki, B. Kirchner

published in

NIC Symposium 2016
K. Binder, M. Müller, M. Kremer, A. Schnurpfeil (Editors)

Forschungszentrum Jülich GmbH,
John von Neumann Institute for Computing (NIC),
Schriften des Forschungszentrums Jülich, NIC Series, Vol. 48,
ISBN 978-3-95806-109-5, pp. 117.
http://hdl.handle.net/2128/9842

Ab Initio Molecular Dynamics Simulations of Ionic Liquids

Martin Thomas, Iris Sancho Sanz, Oldamur Hollóczki, and Barbara Kirchner

Mulliken Center for Theoretical Chemistry, Rheinische Friedrich-Wilhelms-Universität Bonn,
Beringstraße 4, 53115 Bonn, Germany
E-mail: kirchner@thch.uni-bonn.de

We present *ab initio* molecular dynamics simulations of the ionic liquids 1-butyl-3-methylimidazolium trifluoromethanesulfonate and 1-butyl-1-methylpyrrolidinium trifluoromethanesulfonate. We compare the trajectories regarding the formation of hydrogen bonds and the microheterogeneity due to polar and nonpolar phases.

1 Introduction

In the last decades, ionic liquids (ILs) became an extensively investigated type of substances due to their excellent properties as solvents that allow for a wide range of interesting applications[1–3]. The structure of ILs is governed by a large variety of interaction forces such as electrostatic attraction and repulsion[4], dispersion interaction[5,6], and directional atom contacts as in hydrogen bonds[7,8]. A theoretical model has to take into account all these effects to be able to make reasonable predictions about the properties of ILs[9]. On the one hand, static quantum chemical calculations, which explicitly treat the electronic structure of the system on the basis of the Schrödinger equation, can accurately describe the wide range of interaction forces for a particular molecular configuration. On the other hand, molecular dynamics simulations, which rely on empirical force fields to propagate the atoms in the system according to classical mechanics, are able to provide insight into the highly dynamic nature of the interaction network. To benefit from the advantages of both approaches, they can be combined in *ab initio* molecular dynamics (AIMD)[10,11], where classical mechanics is used to describe the propagation of the atoms, but a quantum chemical electronic structure method is employed to obtain the forces. Due to its good cost-performance ratio, density functional theory (DFT) is usually applied for this purpose today. Still, such AIMD simulations require very large computational resources and, thus, they are often carried out in supercomputing facilities.

In this article, we present AIMD simulations of two ILs: 1-butyl-3-methylimidazolium trifluoromethanesulfonate ($[\mathrm{Bmim}][\mathrm{OTf}]$) and 1-butyl-1-methylpyrrolidinium trifluoromethanesulfonate ($[\mathrm{Bmpyrr}][\mathrm{OTf}]$). After a description of the computational setup in Sec. 2, we analyse the trajectories in Sec. 3. In particular, we compare these two ILs regarding the formation of hydrogen bonds by investigating radial distribution functions (RDFs) and combined distribution functions (CDFs). Furthermore, we apply our recently developed domain analysis[12] to study the microheterogeneity, which is a known property of ILs due to the segregation of polar and nonpolar phases on a microscopic level[13].

2 Computational Details

For both ILs, 32 ion pairs were simulated under periodic boundary conditions (see Fig. 1 for representative snapshots of the simulations cells). The AIMD was performed using

	[Bmim][OTf]	[Bmpyrr][OTf]
Composition	32 [Bmim][OTf]	32 [Bmpyrr][OTf]
Cell size (pm)	2281.4	2313.5
Density (g/cm^3)	1.29	1.25
Equilibration time (ps)	5.0	5.0
Physical time (ps)	77.0	74.0

Table 1. Simulation parameters.

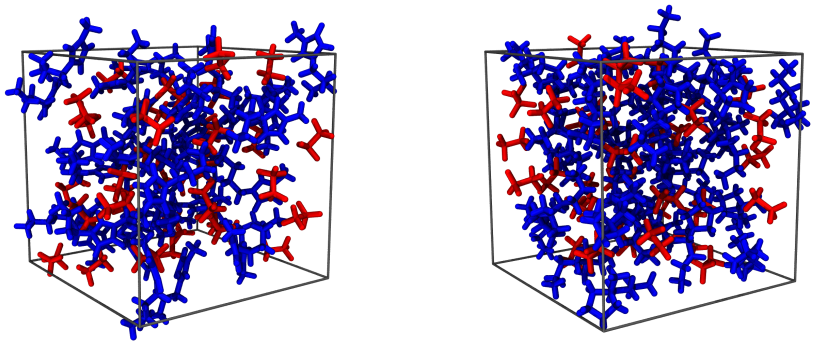

Figure 1. Representative snapshots of the simulation cells; left: [Bmim][OTf], right: [Bmpyrr][OTf], blue: cations, red: anions.

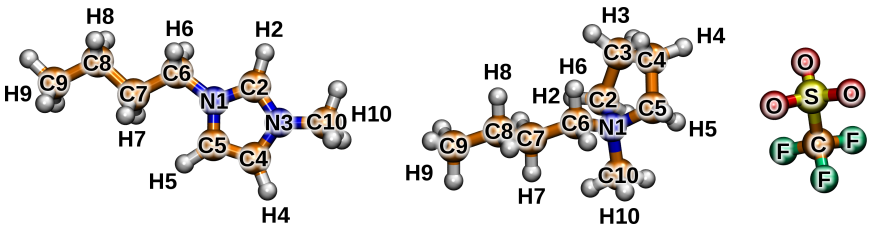

Figure 2. Atom numbering of $[Bmim]^+$, $[Bmpyrr]^+$, and $[OTf]^-$ used throughout this article.

the CP2K program package[14,15]. DFT was employed as electronic structure method, utilising the BLYP exchange-correlation functional[16,17] with Grimme's dispersion correction D3[18]. The molecularly optimised double-zeta basis set MOLOPT-DZVP-SR-GTH[19] was applied to all atoms together with the corresponding Goedecker–Teter–Hutter pseudopotentials[20–22] and a plane wave cutoff of 280 Ry. A timestep of 0.5 fs was chosen, and the temperature was adjusted to 350 K by a Nosé–Hoover chain thermostat[23–25]. The sizes of the cubic simulation cells, the resulting densities, and the simulation times are shown in Tab. 1. The trajectories were analysed using our trajectory analysis software package TRAVIS[26,12,27]. The atom numbering to present the results is given in Fig. 2.

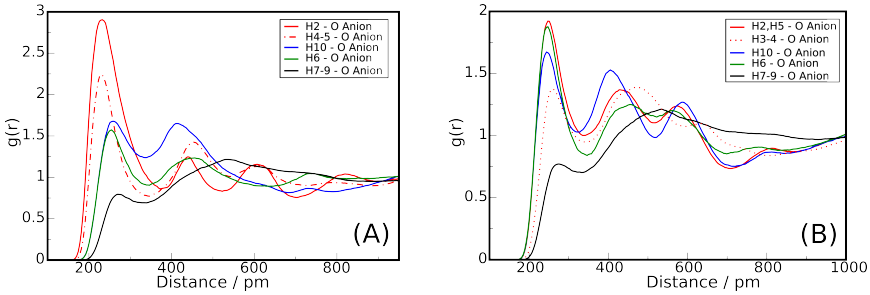

Figure 3. Radial distribution functions between hydrogen atoms of the cation and oxygen atoms of the anion for [Bmim][OTf] (A) and [Bmpyrr][OTf] (B).

The starting structures for the AIMD simulations were created by classical molecular dynamics carried out using LAMMPS[28]. Force constants for bonds, angles, dihedral angles, and improper torsions, as well as Lennard-Jones parameters were taken from the general AMBER force field[29] and from the force field for imidazolium-based ILs by Liu *et al.*[30] Atomic partial charges for electrostatic interactions were derived from a restrained electrostatic potential fit[31]. The AIMD simulations were equilibrated by massive thermostatting with a coupling time constant of 10 fs for about 2.5 ps and running with a single thermostat chain for additional 2.5 ps. During the second equilibration phase and in the production run, the thermostat coupling time constant was set to 100 fs.

3 Results and Discussion

On the basis of the RDFs, for the [Bmim][OTf] IL, the most intense interaction is coordinated through the ring hydrogen atoms (see Fig. 3 (A)). The most acidic one, placed between the two nitrogen atoms (H2), is the biggest, presenting an intensity of 2.9 for a H–O bond distance of 230.6 pm. This is followed by the other two hydrogen atoms of the ring (H4–5) which present a similar peak with an intensity of 2.2 at a H–O distance of 228.4 pm. The hydrogen atoms of the methyl residue (H10), as well as those from the first carbon atom of the butyl chain (H6) also show sizable peaks with intensities of 1.7 and 1.6, respectively, and longer H–O distances of 257.1 pm for H10 and 256.0 pm for H6. Thus, applying the criteria established by G. A. Jeffrey[32], the two first hydrogen bonds from H2 and H4–5 could be considered of medium strength, with an interaction type mostly electrostatic, and the ones where H10 and H6 are the donors are weak hydrogen bonds with an electrostatic interaction type. When looking into the RDFs of [Bmpyrr][OTf], the most intense interaction is also observed through the ring hydrogen atoms close to the nitrogen atom (H2, H5) with a H–O distance of 248.8 pm (see Fig. 3 (B)), following, as above, the rule "Better acid – Better donor"[33], although its intensity of only 1.9 is one unit less than the one depicted by the H2 of $[Bmim]^+$. The hydrogen atoms of the first position in the butyl chain (H6) present almost the same peak with an intensity of 1.9 and a distance of 246.3 pm for the hydrogen bond. Finally, the methyl hydrogen atoms (H10) (see Fig. 3 (B)) are better donors than the other ring hydrogen atoms (H3, H4) with a H–O distance 15 pm shorter (244 pm *vs.* 259 pm) and 0.3 more intense (1.7 *vs.* 1.4). The four interac-

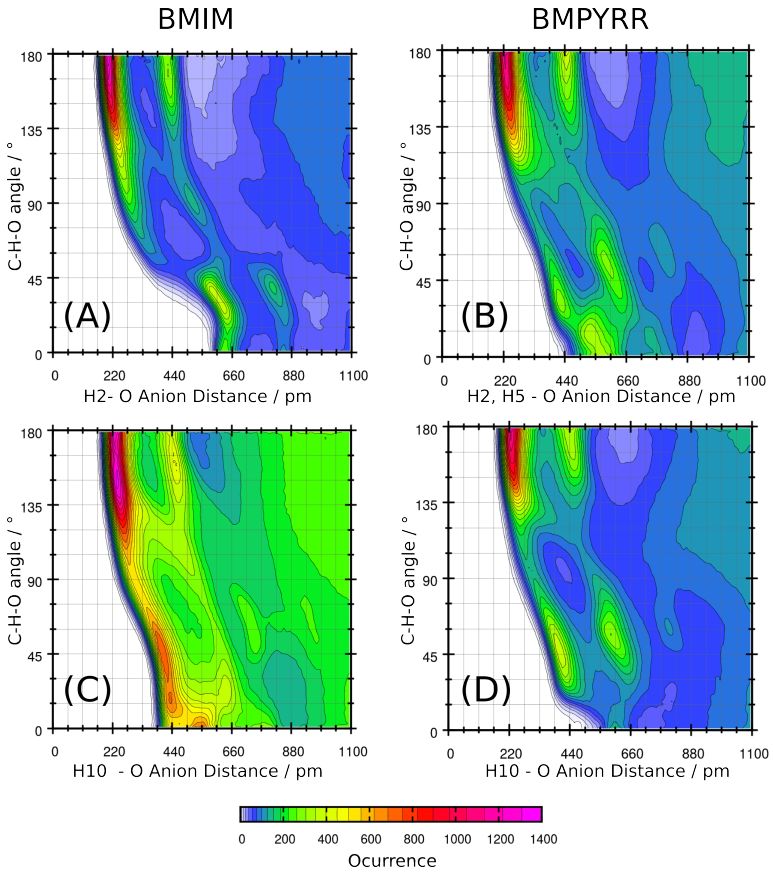

Figure 4. Combined distribution functions showing C–H–O angles against the corresponding H–O distances for $[\mathrm{Bmim}][\mathrm{OTf}]$ (A, C) and $[\mathrm{Bmpyrr}][\mathrm{OTf}]$ (B, D).

tions considered here are of an electrostatic nature, leading to weak hydrogen bonding[32]. The acidity of the hydrogen bond donor can be related to the $\mathrm{p}K_\mathrm{a}$ of the donor molecule. It is known that electron-withdrawing groups enhance the donor strength, as it opens the possibility of a cooperation through double bonds (namely, π cooperativity) as is shown by *o*-nitrophenol or formamide, just to mention some[33]. Having these two concepts in mind, it is easy to understand our results: in the $[\mathrm{Bmpyrr}]^+$ cation, which has no aromaticity, the hydrogen atoms H2, H5, H10, and H6 are two bonds away of the electronegative nitrogen atom while H3 and H4 are three bonds away. In the case of the $[\mathrm{Bmim}]^+$ cation, the ring aromaticity allows the π cooperativity, enhancing the hydrogen bond ability of the ring hydrogen atoms.

According to the CDFs, the oxygen atoms of the triflate anion are oriented almost 180° towards the most acidic ring hydrogen atoms, both in $[\mathrm{Bmim}][\mathrm{OTf}]$ (H2) and in $[\mathrm{Bmpyrr}][\mathrm{OTf}]$ (H2, H5) (see Fig. 4 (A, B)). In the CDF corresponding to the hydrogen bond between H2 in $[\mathrm{Bmim}]^+$ and the oxygen atoms in the anion (Fig. 4 (A)) we see

the highest occurrence at a distance of $215\,\mathrm{pm}$ and a linear angle corresponding with the oxygen pointing towards H2. This peak has a neighbour with a H2–O distance of $438\,\mathrm{pm}$ and a hydrogen bond angle of $180°$ too which corresponds to the other two oxygen atoms in the triflate anion. With a bond distance of $620\,\mathrm{pm}$ we encounter another peak showing C2–H2–O angles between $0°$ and $45°$, these ones correspond to distances and angles between H2 and oxygen atoms that are coordinated to H4 and H5, almost coplanar with H2. At a distance of around $825\,\mathrm{pm}$ we can see the neighbour of this peak, with almost the same range of angles and less occurrence. H2 and H5 in $[\mathrm{Bmpyrr}]^+$ (Fig. 4 (B)) present a similar CDF but with less definite peaks. The one with the highest intensity can be seen at a H–O distance of $230\,\mathrm{pm}$ and an angle of $180°$. The other two oxygen atoms of the triflate anion are reflected in the neighbour peak at $440\,\mathrm{pm}$, which presents even less intensity. Another interaction with angles between $0°$ and $45°$ can also be observed in this graph with irregular peaks that blend together due to the variety of hydrogen atoms H3–4. These peaks, as seen above, clearly show the distances and angles of an oxygen atom coordinated to H3 or H4. The CDFs plotting the hydrogen bonds formed with H10 are shown in Fig. 4 (C, D). The peaks in $[\mathrm{Bmim}][\mathrm{OTf}]$ are less distinct and this can be related to the flexibility of C10 and H10 and the weaker hydrogen bonding. The most intense peak appears at a H10–O distance of around $220\,\mathrm{pm}$ and with a C10–H10–O angle between $135°$ and $180°$. The second peak in occurrence, which has almost the half of the first one, appears at around $430\,\mathrm{pm}$ in the H10–O distance and with an angle between $75°$ and $0°$ corresponding to the other hydrogen atoms of the same methyl group. In the $[\mathrm{Bmpyrr}]^+$ plot (D), the peaks are much more distinct. The highest peak is shown at a H10–O distance of around $220\,\mathrm{pm}$ and angles between $140°$ and $180°$ with a secondary peak due to the other two oxygen atoms with the same angle and at around $440\,\mathrm{pm}$. The second peak in intensity can be seen at $430\,\mathrm{pm}$ with an angle between $90°$ and $15°$, corresponding to the other hydrogen atoms of the same methyl group again.

The results of the domain analysis are shown in Tab. 2. In both ILs, the nonpolar domains are defined as the butyl chains without the methylene group connected to the ring, so they contain the carbon atoms C7, C8, and C9 with the attached hydrogen atoms, while the polar domains consist of all other atoms. Both ILs show a similar behaviour: the polar moieties form one single domain during the whole simulations, but the nonpolar side chains are sometimes split into several distinct domains, leading to average domain counts of 1.33 and 1.16, respectively. This indicates that the polar groups form an extended network that ranges through the whole simulation cells while the butyl chains tend to form aggregates in between. It has to be noted that a system size of 32 ion pairs is too small to fully observe this aggregation of the nonpolar side chains. The interpretation is supported by the neighbour matrices in Tab. 3 and Tab. 4, which show the average contact area and the average neighbour count between different groups. For this purpose, the polar domains are split into the anions and the head groups of the cations ("ring"). It is clearly apparent that the cations' rings are primarily surrounded by anions and *vice versa*, supporting the picture that they form an extended network which is stabilised by hydrogen bonding. The self contacts of the side chains seem to be quite low, but it has to be kept in mind that a certain contact area to the rings and the anions the latter interacts with is simply enforced due to the covalent bond.

Domain	IL	n	V / Å^3	A / Å^2
Polar	[Bmim][OTf]	1.00	8813	3259
	[Bmpyrr][OTf]	1.00	9434	3155
Nonpolar	[Bmim][OTf]	1.33	2568	2734
	[Bmpyrr][OTf]	1.16	2718	2907

Table 2. Domain analysis in [Bmim][OTf] and [Bmpyrr][OTf]: average number of domains n, average domain volume V, and average domain surface area A.

	Anion	Ring	Nonpolar
Anion	18.6 (4.1)	89.8 (6.1)	48.2 (5.4)
Ring	89.8 (6.1)	31.5 (5.2)	53.7 (5.1)
Nonpolar	48.2 (5.4)	53.7 (5.1)	25.4 (3.2)

Table 3. Neighbour matrix in [Bmim][OTf]: average contact areas in Å^2, neighbour counts in parentheses.

	Anion	Ring	Nonpolar
Anion	18.3 (3.5)	92.7 (6.1)	43.7 (5.0)
Ring	92.7 (6.1)	40.5 (5.7)	54.9 (5.0)
Nonpolar	43.7 (5.0)	54.9 (5.0)	24.6 (3.1)

Table 4. Neighbour matrix in [Bmpyrr][OTf]: average contact areas in Å^2, neighbour counts in parentheses.

4 Conclusion

We have presented a study of the ILs [Bmim][OTf] and [Bmpyrr][OTf] in which we show how the cations' rings are surrounded by anions and *vice versa*. The strongest hydrogen bond is formed between H2 and O in [Bmim][OTf]. Every other polar hydrogen in the cation coordinates to the oxygen with less intensity and larger distances. Due to the π cooperativity the hydrogen bonds formed in $[\mathrm{Bmim}]^+$ are more intense than those formed in the analogous $[\mathrm{Bmpyrr}]^+$ IL which presents no aromaticity in its heterocyclic ring. The domain analysis indicates a similar degree of microheterogeneity in both ILs due to the aggregation of the butyl chains, but larger system sizes would be needed to observe this effect more clearly.

Acknowledgements

We gratefully acknowledge the allocation of computer time by the Jülich Supercomputing Centre. B.K. would like to thank the Deutsche Forschungsgemeinschaft (DFG) for support under the SPP 1708 project KI768/12-1.

References

1. T. Welton, *Room-Temperature Ionic Liquids. Solvents for Synthesis and Catalysis*, Chem. Rev., **99**, no. 8, 2071–2084, 1999.
2. N. V. Plechkova and K. R. Seddon, *Applications of ionic liquids in the chemical industry*, Chem. Soc. Rev., **37**, 123–150, 2008.
3. J. P. Hallett and T. Welton, *Room-Temperature Ionic Liquids: Solvents for Synthesis and Catalysis. 2*, Chem. Rev., **111**, no. 5, 3508–3576, 2011.
4. S. Tsuzuki, H. Tokuda, and M. Mikami, *Theoretical analysis of the hydrogen bond of imidazolium C2-H with anions*, Phys. Chem. Chem. Phys., **9**, 4780–4784, 2007.
5. S. Zahn, F. Uhlig, J. Thar, C. Spickermann, and B. Kirchner, *Intermolecular Forces in an Ionic Liquid ([Mmim][Cl]) versus Those in a Typical Salt (NaCl)*, Angew. Chem. Int. Ed., **47**, no. 19, 3639–3641, 2008.
6. S. Grimme, W. Hujo, and B. Kirchner, *Performance of dispersion-corrected density functional theory for the interactions in ionic liquids*, Phys. Chem. Chem. Phys., **14**, 4875–4883, 2012.
7. S. B. C. Lehmann, M. Roatsch, M. Schöppke, and B. Kirchner, *On the physical origin of the cation-anion intermediate bond in ionic liquids Part I. Placing a (weak) hydrogen bond between two charges*, Phys. Chem. Chem. Phys., **12**, 7473–7486, 2010.
8. M. Brehm, H. Weber, A. S. Pensado, A. Stark, and B. Kirchner, *Proton transfer and polarity changes in ionic liquid-water mixtures: a perspective on hydrogen bonds from ab initio molecular dynamics at the example of 1-ethyl-3-methylimidazolium acetate-water mixtures-Part 1*, Phys. Chem. Chem. Phys., **14**, 5030–5044, 2012.
9. B. Kirchner, O. Hollóczki, J. N. Canongia Lopes, and A. A. H. Pádua, *Multiresolution calculation of ionic liquids*, WIREs Comput. Mol. Sci., **5**, no. 2, 202–214, 2015.
10. D. Marx and J. Hutter, *Ab Initio Molecular Dynamics: Basic Theory and Advanced Methods*, Cambridge University Press, 2009.
11. B. Kirchner, P. J. Dio, and J. Hutter, "Real-world predictions from ab initio molecular dynamics simulations", in: Multiscale Molecular Methods in Applied Chemistry, Barbara Kirchner and Jadran Vrabec, (Eds.), vol. 307 of *Top. Curr. Chem.*, pp. 109–153. Springer Berlin Heidelberg, 2012.
12. M. Brehm, H. Weber, M. Thomas, O. Hollóczki, and B. Kirchner, *Domain Analysis in Nanostructured Liquids: A Post-Molecular Dynamics Study at the Example of Ionic Liquids*, ChemPhysChem, 2015.
13. R. Hayes, G. G. Warr, and R. Atkin, *Structure and Nanostructure in Ionic Liquids*, Chem. Rev., **115**, no. 13, 6357–6426, 2015.
14. J. VandeVondele, M. Krack, F. Mohamed, M. Parrinello, T. Chassaing, and J. Hutter, *QUICKSTEP: Fast and accurate density functional calculations using a mixed Gaussian and plane waves approach*, Comput. Phys. Commun., **167**, no. 2, 103–128, 2005.
15. J. Hutter, M. Iannuzzi, F. Schiffmann, and J. VandeVondele, *CP2K: atomistic simulations of condensed matter systems*, WIREs Comput. Mol. Sci., **4**, no. 1, 15–25, 2014.
16. A. D. Becke, *Density-functional exchange-energy approximation with correct asymptotic behavior*, Phys. Rev. A, **38**, 3098–3100, Sep 1988.

17. C. Lee, W. Yang, and R. G. Parr, *Development of the Colle-Salvetti correlation-energy formula into a functional of the electron density*, Phys. Rev. B, **37**, 785–789, Jan 1988.
18. S. Grimme, J. Antony, S. Ehrlich, and H. Krieg, *A consistent and accurate ab initio parametrization of density functional dispersion correction (DFT-D) for the 94 elements H-Pu*, J. Chem. Phys., **132**, no. 15, 154104, 2010.
19. J. VandeVondele and J. Hutter, *Gaussian basis sets for accurate calculations on molecular systems in gas and condensed phases*, J. Chem. Phys., **127**, no. 11, 114105, 2007.
20. S. Goedecker, M. Teter, and J. Hutter, *Separable dual-space Gaussian pseudopotentials*, Phys. Rev. B, **54**, 1703–1710, Jul 1996.
21. C. Hartwigsen, S. Goedecker, and J. Hutter, *Relativistic separable dual-space Gaussian pseudopotentials from H to Rn*, Phys. Rev. B, **58**, 3641–3662, Aug 1998.
22. M. Krack, *Pseudopotentials for H to Kr optimized for gradient-corrected exchange-correlation functionals*, Theor. Chem. Acc., **114**, 145–152, 2005.
23. S. Nosé, *A unified formulation of the constant temperature molecular dynamics methods*, J. Chem. Phys., **81**, no. 1, 511–519, 1984.
24. S. Nosé, *A molecular dynamics method for simulations in the canonical ensemble*, Mol. Phys., **52**, no. 2, 255–268, 1984.
25. G. J. Martyna, M. L. Klein, and M. Tuckerman, *Nosé–Hoover chains: The canonical ensemble via continuous dynamics*, J. Chem. Phys., **97**, no. 4, 2635–2643, 1992.
26. M. Brehm and B. Kirchner, *TRAVIS – A Free Analyzer and Visualizer for Monte Carlo and Molecular Dynamics Trajectories*, J. Chem. Inf. Model., **51**, no. 8, 2007–2023, 2011.
27. "TRAVIS – Trajectory Analyzer and Visualizer", `http://www.travis-analyzer.de`.
28. S. Plimpton, *Fast Parallel Algorithms for Short-Range Molecular Dynamics*, J. Comput. Phys., **117**, no. 1, 1–19, 1995.
29. J. Wang, R. M. Wolf, J. W. Caldwell, P. A. Kollman, and D. A. Case, *Development and testing of a general Amber force field*, J. Comput. Chem., **25**, no. 9, 1157–1174, 2004.
30. Z. Liu, S. Huang, and W. Wang, *A Refined Force Field for Molecular Simulation of Imidazolium-Based Ionic Liquids*, J. Phys. Chem. B, **108**, no. 34, 12978–12989, 2004.
31. U. C. Singh and P. A. Kollman, *An approach to computing electrostatic charges for molecules*, J. Comput. Chem., **5**, no. 2, 129–145, 1984.
32. G. A. Jeffrey, *An Introduction to Hydrogen Bonding*, Oxford University Press, 1997.
33. P. Gilli, L. Pretto, V. Bertolasi, and G. Gilli, *Predicting Hydrogen-Bond Strengths from Acid–Base Molecular Properties*, Acc. Chem. Res., **42**, no. 1, 33–44, 2009.